

Rational Design of a Tripodal Ligand for U(IV): Synthesis and Characterization of a U–Cl Species and Insights into Its Reactivity

Kang Liu,[†] Ji-Pan Yu,[†] Qun-Yan Wu, Xue-Bing Tao, Xiang-He Kong, Lei Mei,^{*} Kong-Qiu Hu, Li-Yong Yuan, Zhi-Fang Chai, and Wei-Qun Shi^{*}



Cite This: <https://dx.doi.org/10.1021/acs.organomet.0c00638>



Read Online

ACCESS |



Metrics & More

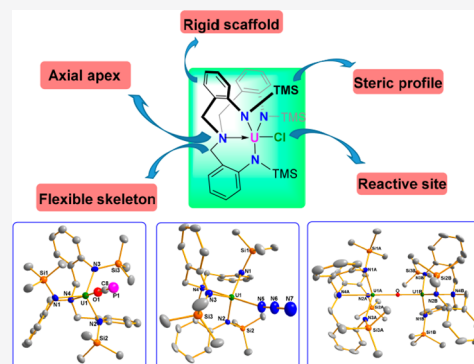


Article Recommendations



Supporting Information

ABSTRACT: The rational design and synthesis of the Trapen ligand (**1**, tris(2-aminobenzyl)amine) with a tripodal scaffold is reported. Treatment of Trapen with *n*-BuLi and TMSCl results in the formation of the corresponding complex [(Trapen^{TMS})(Li)₃] (**2**). In particular, **2** reacts with UCl₄ to give the important synthon uranium(IV) complex [U(Trapen^{TMS})(Cl)] (**3**) with all of the nitrogen atoms bound to the uranium(IV) center. Moreover, the pseudohalogen congener [U(Trapen^{TMS})(OCP)] (**4**) or the azide analogue [U(Trapen^{TMS})(N₃)] (**5**) could be obtained when [U(Trapen^{TMS})(Cl)] (**3**) was treated with NaOCP(dioxane)_{2,5} or NaN₃ by a salt metathesis approach. In addition, the reaction of KC₈ with [U(Trapen^{TMS})(Cl)] (**3**) did not afford the desired U(III) complex but produced the unexpected bridging diuranium oxo complex [U(Trapen^{TMS})₂(μ-O)] (**6**). All of the compounds were isolated in the solid state and characterized by NMR, X-ray crystal diffraction, and FT-IR, and UV–vis–NIR as well as elemental analyses and SQUID magnetization measurements. The combined experimental analyses and chemical calculations support all of the formal uranium(IV) species.



INTRODUCTION

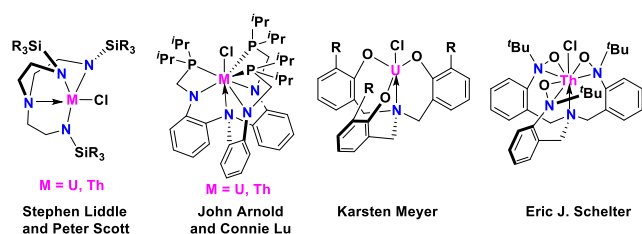
Nonaqueous molecular actinide chemistry is a challenging yet vital frontier realm that has flourished in recent years.¹ As we know, uranium is the fundamental resource of nuclear energy and is readily available with a specific low activity, the in-depth study of which has profoundly enhanced our understanding of the roles of the valence orbitals in covalent interactions, since the issue of covalency remains an important scientific subject of debate to date. Therefore, to elucidate the principal problems regarding trends of valence orbitals in chemical bonding and reactivity toward uranium, a further accurate investigation and exploration of landmark species is necessary, thus providing reliable evidence.

Polydentate ligands, especially tetradentate ligands with a tripodal topology as the linkages, have attracted a great deal of attention due to their widespread utility in synthetic performance available toward actinide complexes.^{2–13} We considered that three main features meet the demands of actinide coordination chemistry: (a) tripodal ligands play a key role in enforcing single-site reactivity to a metal center upon coordination; (b) steric arguments account for the variability of reaction, and specifically, substituent groups incorporated into the side arm of the tripodal ligands help to adjust steric resistance and endow the tailored tripodal ligands with striking features for addressing the specific issues; (c) the ligand unit provides a pocket scaffold for immobilizing the reactive actinide precursor because of saturation of the coordination

sphere, while avoiding decomposition processes for the formation of a supported structure. Thus, it is well-known that a tripodal ligand systematically influences the stability, compatibility, and reactivity of uranium complexes. Over the past decade, Liddle,^{14–31} Arnold,⁶ and Meyer^{32–44} have contributed much to the diversity and progress of the organometallic chemistry of actinides by the family of tripodal ligands, including actinide–metal bonds,^{10,45–48} actinide–ligand multiple bonds,^{14,15,18,21,30,31} small-molecule activation,^{26,44,49–51} lower oxidation states of actinides,^{39,40} and so on. More recently, Schelter et al.⁵² have demonstrated that a tripodal nitroxide ligand framework could be used to synthesize and characterize a series of Th(IV)–imido complexes (Scheme 1). Actually, the reactivity is generally ligand dependent, and no all-purpose ligand has yet been manifested in dealing with all of the challenges in chemical bonding transformations, because imperceptible adjustments in the steric, geometrical, and/or electronic character of the ligands can give rise to tremendous changes in bonding and reactivity. It is worth noting that conformationally rigid and

Received: September 24, 2020

Scheme 1. Representative Examples of Actinide Complexes with Tripodal Skeletons



locally flexible frameworks could provide additional advantages for fine-tuning the ligand rigidity and pliability.⁴ Therefore, we have begun to design and synthesize novel ligands that would provide a platform for evaluating uranium precursor reactivity and further enhancing our understanding of the extent of covalency in uranium–ligand bonding.

Here, previous work triggered our efforts to synthesize a new tris(2-aminobenzyl)amine proligand, Trapen, via a multistep synthesis strategy. The Trapen ligand is an excellent ligand transfer reagent that can be conveniently converted to the corresponding Trapen U(IV)–Cl complex, which is an important uranium precursor. Furthermore, the Trapen U(IV)–Cl complex has found utility as a precursor to U(IV)–OCP, U(IV)–N₃, and the unexpected uranium(IV) bridging oxygen complex $[\{U(\text{Trapen}^{\text{TMS}})\}_2(\mu\text{-O})]$ by salt elimination or treatment over K₂C₈, respectively. The centrally located amine serves as the anchor apex with axial electronic stabilization, thus providing a platform for sterically encumbering one side of the uranium site. The TMS groups of the arylamine generally introduce pendent arms and generate a well-defined pocket around the uranium to optimize the reactivity. Complexes 3–6 have been comprehensively characterized by crystallography, multinuclear NMR and FT-IR, UV–vis–NIR, variable-temperature SQUID magnetometry, and elemental analyses.

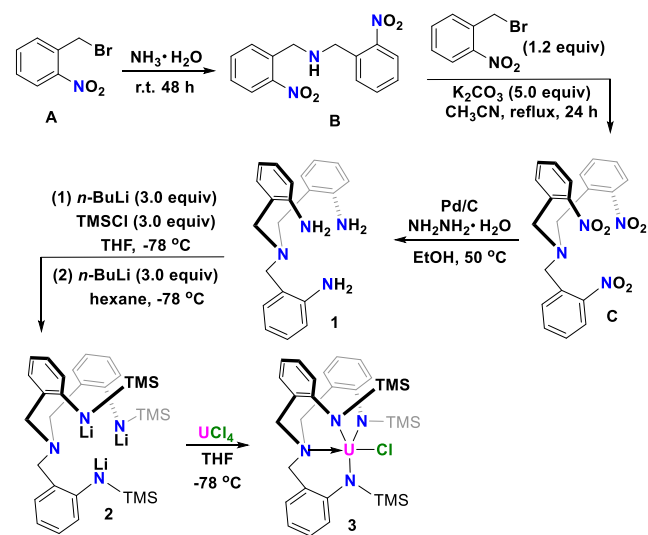
RESULTS AND DISCUSSION

Synthesis and Characterization of Trapen Ligand 1.

The whole synthetic approach required a stepwise preparation strategy (Scheme 2). The key intermediate, 2-((bis(2-aminobenzyl)amino)methyl)aniline (**1**), was prepared in three simple steps in 55% yield from the commercially available starting material 1-(bromomethyl)-2-nitrobenzene. The detailed process is as follows. Treatment of commercial 1-(bromomethyl)-2-nitrobenzene (**A**) with excess ammonia afforded the bis(2-nitrobenzyl)amine **B** as a yellow powder in 71% isolated yield. Treatment of **B** with 1.2 equiv of 1-(bromomethyl)-2-nitrobenzene, followed by the addition of 5 equiv of K₂CO₃ as a base with reflux for 24 h afforded tris(2-nitrobenzyl)amine (**C**) as a pale yellow solid in 87% yield. The synthesis of Trapen (**1**) was carried out by reduction of **C** using hydrazine with a catalytic amount of Pd/C at 50 °C for 0.5 h. This protocol provides an efficient and practical method for construction of the Trapen ligand, although a typical procedure has been reported previously.⁵³ The structures of all the newly synthesized compounds were identified on the basis of ESI-MS, ¹H NMR, and ¹³C NMR spectral data. The simple preparation and synthetic feasibility provide promising potential exploitation.

Synthesis and Characterization of 3. Treatment of Trapen with 3 equiv of *n*-BuLi followed by addition of 3 equiv

Scheme 2. General Procedure for Synthesis of the Trapen Ligand and Uranium(IV) Complex [U(Trapen^{TMS})(Cl)]



of TMSCl and once again with 3 equiv of *n*-BuLi resulted in formation of the corresponding complex $[(\text{Trapen}^{\text{TMS}})(\text{Li})_3]$ (**2**) in good yield (71%). The complex U(Trapen^{TMS})Cl (**3**) was synthesized in moderate (62%) yield by adding a THF solution of the readily available (Trapen^{TMS})(Li)₃ (**2**) to a –78 °C THF solution of UCl₄ along with elimination of LiCl (Scheme 2), analogously to Tren uranium(IV) chloride complexes. Removal of the solvent and extraction by hot toluene furnished a black solution, which was recrystallized to provide **3** in 62% yield. The ¹H nuclear magnetic resonance (NMR) spectrum of **3** recorded in C₆D₆ at 25 °C spans the range –6 to +20 ppm with seven resonances. The relatively intense and sharp signal at –6.61 ppm is assigned to TMS groups on the arylamine pendant arm. The ²⁹Si NMR spectrum of **3** exhibits a single peak at –148.69 ppm, indicating only one silicon chemical environment on the NMR time scale.⁵⁴ The solid-state structure of **3** was illustrated by an X-ray diffraction study (Figure 1a). For the five-coordinate complex **3**, the calculated τ_5 value is 0.83,⁵⁵ which indicates that the uranium center adopts a distorted-trigonal-bipyramidal geometry where both nitrogen atoms are coordinated to the uranium, forming three six-membered rings. The U–N_{amido} bond lengths, including U1–N1, U1–N2, U1–N3 bonds, are 2.244(6), 2.244(6) and 2.225(6) Å, respectively, which are unexceptional.⁵⁶ The U–N_{amine} bond distance in **3** (U1–N4 = 2.631(6) Å) lies in the range of values for previously reported and structurally ascertained U(IV)–amine complexes^{5,57} and is moderately longer than the average U–N_{amido} bond distance in **3** (average U–N = 2.237(6) Å). The U1–Cl1 bond length is 2.644(2) Å, which is within the sum of the covalent radii of 2.69 Å, in accordance with previous work on uranium(IV)–Cl bond lengths with other ligands.^{5,6} A SQUID magnetic moment measurement was conducted to study the temperature-dependent behavior of the tetravalent uranium. The magnetic moment of **3** is 3.18 μ_B at 300 K and decreases more sharply below 50 K to 0.58 μ_B at 2 K and tends to zero. This experimental phenomenon reflects that uranium(IV) is a magnetic singlet at low temperature with a temperature-independent paramagnetism (TIP) characteristic (Figure 2).⁵⁸ The UV/vis/NIR spectrum of **3** is typical of 5f² uranium(IV), with low-intensity peaks across the region

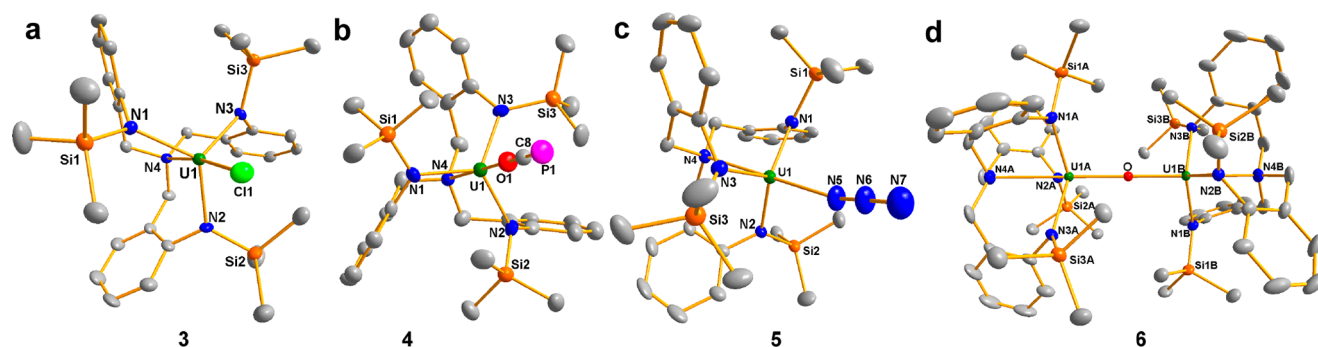


Figure 1. Solid-state structures of **3** (a), **4** (b), **5** (c) and **6** (d) by X-ray crystallography with 50% probability ellipsoids. Hydrogen atoms are omitted for clarity. Selected experimental bond distances (Å) and angles (deg): for **3**, U1–Cl1 2.644(2), U1–N1 2.244(6), U1–N2 2.244(6), U1–N3 2.225(6), U1–N4 2.631(6), N1–U1–Cl1 99.79(16), N2–U1–Cl1 106.07(16), N3–U1–Cl1 94.83(17), N4–U1–Cl1 172.87(15), N3–U1–N1 122.8(2), N3–U1–N2 115.8(2), N2–U1–N1 112.5(2). $\tau_5(\text{U}) = 0.83$; for **4**, U1–N1 2.230(5), U1–N4 2.660(12), U1–O1 2.257(10), O1–C8 1.262(14), C8–P1 1.549(13), N4–U1–O1 180.0, O1–C8–P1 180.0; for **5**, U1–N1 2.245(4), U1–N2 2.244(4), U1–N3 2.230(4), U1–N4 2.621(4), U1–N5 2.293(4), N5–N6 1.178(6), N6–N7 1.124(7), N4–U1–N5 175.90(16), N5–N6–N7 176.4(8); for **6**, U1A–N1A 2.280(4), U1A–N4A 2.750(7), U1A–O1 2.132(3), N4A–U1A–O1 180.0, U1A–O1–U1B 180.0. Color code: uranium, bottle green; phosphorus, violet; oxygen, red; nitrogen, blue; chloride, green; carbon, grey.

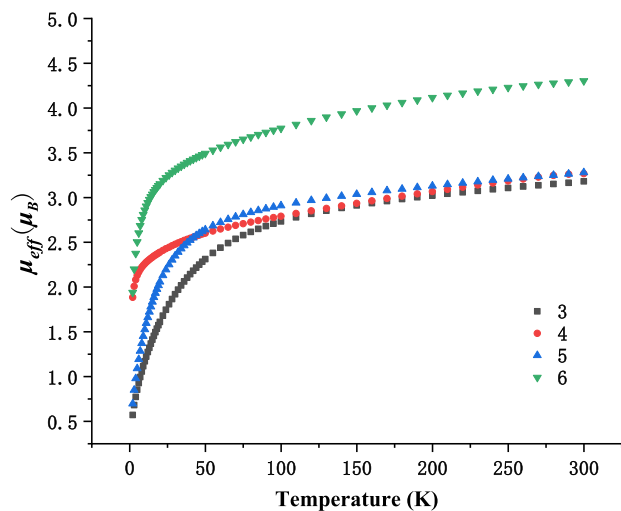
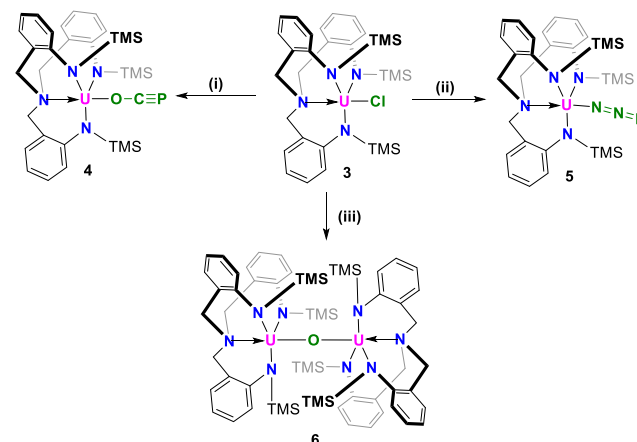


Figure 2. Variable-temperature SQUID magnetic moments μ_B for **3–6** over the temperature range 2–300 K.

500–2000 nm ($\epsilon = 5\text{--}30 \text{ M}^{-1} \text{ cm}^{-1}$) (Figure S2). With regard to the electrochemical behavior of **3**, an electrochemical irreversible one-electron process at $E_{1/2} = -2.3 \text{ V}$ (vs $\text{Fc}^{0/+}$) for the $[\text{U}^{\text{IV}}]/[\text{U}^{\text{III}}]$ redox couple is observed by means of a cyclic voltammetry experiment in THF (0.5 M $[\text{N}^{\text{tBu}}_4][\text{PF}_6]$ supporting electrolyte) (Figure S3). In order to better define the steric influence caused by $[\text{U}(\text{Trapen})(\text{Cl})]$ and $[\text{U}(\text{Tren})(\text{Cl})]$, a percent buried volume calculation was performed using a web application.^{59–61} It appears that when 5 Å is selected as the value for the sphere radius, the final calculation result for the order of steric hindrance is as follows: $[\text{Tren}^{\text{TIPS}}]^{3-}$ (buried volume: 76.2%) > $[\text{Trapen}^{\text{TMS}}]^{3-}$ (buried volume: 74.9%) > $[\text{Tren}^{\text{TMS}}]^{3-}$ (buried volume: 60.6%) (Figure S4). In comparison to Tren^{TMS} -supported U(IV)–Cl complexes, a notable feature of **3** is that there is no coordinated THF located in the uranium center as well as no bridging chloride center in $\text{Trapen}^{\text{TMS}}$ ligand, which is a sterically demanding feature while affording a single coordination architecture to increase the reactivity. Furthermore, it has been indicated that $\text{U}(\text{Trapen}^{\text{TMS}})\text{Cl}$ (**3**) as a potential precursor may contribute greatly to challenging issues in organoactinide chemistry.

Synthesis and Characterization of 4–6. To further investigate the synthetic transformation of the excellent synthon **3**, a new class of uranium complexes supported by the tripodal Trapen ligand with apical donors were observed (Scheme 3). The salt metathesis reaction of the precursor **3**

Scheme 3. Synthesis of Uranium Complexes 4–6^a



^aReaction conditions: (i) $\text{NaOCP}(\text{dioxane})_{2.5}$, THF, -78°C to room temperature, 12 h, $-\text{NaCl}$, $-\text{dioxane}$ (2.5 equiv); (ii) NaN_3 , THF, -78°C to room temperature, 12 h, $-\text{NaCl}$; (iii) KC_8 , THF, -78°C to room temperature, 1 h, $-\text{KCl}$, $-\text{graphite}$.

with 1.1 equiv of $\text{NaOCP}(\text{dioxane})_{2.5}$ or commercially available NaN_3 in THF afforded the solvent-free uranium complexes **4** and **5**. The crystal structure of **4** reveals that a phosphoethynolate species is bonded to the uranium center in a U–OCP fashion, ruling out the phosphorus-bonded mode (Figure 1b). The amphiphilic 2-phosphoethynolate anion can bind to the metal center via the phosphorus atom ($^-\text{P}=\text{C}=\text{O}$ moiety) or via the oxygen atom ($^-\text{O}-\text{C}\equiv\text{P}$ moiety). The O–C and C–P distances of 1.262(14) and 1.549(13) Å, respectively, are in agreement with the reported distances (O–C and C–P distances of 1.241(2) and 1.557(2) Å, respectively, in $[\text{U}(\text{Tren}^{\text{TIPS}})(\text{OCP})]$ and O–C and C–P distances of 1.219(6) and 1.576(5) Å, respectively, in $[\text{U}(\text{OCP})(\text{amid})_3]$),^{17,34,62} suggesting that the latter resonance

mode with a negatively charged oxygen atom is favored in comparison to the former mode, as the oxygen atom prefers coordinating to a uranium ion with hard electropositivity. Meanwhile, the crystal structure of **4** reveals a U–O bond length of 2.257(10) Å, which is well in line with the other structurally characterized examples [U(Tren^{TIPS})(OCP)] (2.2942(14) Å) and [U(OCP)(amid)₃] (2.297(3) Å).^{17,62} In comparison to the uranium–chloride bond distance of 2.644(2) Å in **3**, the U–O bond length in **4** is 2.257(10) Å. The U–N_{amine} bond length of 2.660(12) Å in **4** is similar to the corresponding bond length of 2.631(6) Å in **3**. This reflects that the uranium ion resides 0.4265(5) Å above the plane of the three arylamine amide atoms in **4**, while the corresponding displacement of the uranium ion in **3** is 0.3908(4) Å. A variable-temperature SQUID magnetic measurement on a powdered sample of **4** (Figure 2) gives a magnetic moment of 3.26 μ_B at 300 K, which is close to the values for [U(Tren^{TIPS})(OCP)] (3.04 μ_B) and U(OCP)(amid)₃ (amid = *N,N'*-bis(trimethylsilyl)benzamidinate) (3.23 μ_B).^{17,62} However, its magnetic moment decreases to 1.88 μ_B at 2 K, which is appreciably higher in comparison to the reported species.^{17,34} The ¹H NMR chemical shifts of **4** range from –31 to +31 ppm, and the ³¹P NMR spectrum of **4** reveals a resonance at –285 ppm, suggesting a typical 3-fold symmetrical Trapen–uranium(IV) complex. The FT-IR spectrum of **4** has an apparent and strong absorption peak at 1673 cm^{–1}, which is assigned to the C–O stretching vibration of the OCP[–] ligand. However, the broad Trapen signal makes the C–P stretching signal disappear in the region of 1200–1300 cm^{–1} (Figure S5). The UV–vis–NIR electronic absorption spectrum of **4** shows that a charge transfer absorption band is detected in the range of the UV–vis regions, while there are low-intensity peaks in the NIR region due to weak f–f absorptions, which is in agreement with previously reported uranium–OCP complexes (Figure S6).

The crystal structure of **5** reveals U1–N5, N5–N6, and N6–N7 distances of 2.293(4), 1.178(6), and 1.124(7) Å, and N4–U1–N5 and N5–N6–N7 angles of 175.90(16) and 176.4(8), respectively (Figure 1c). Furthermore, the solid-state structure exhibits typical U–N_{amido} and U–N_{amine} distances of 2.240 (av) and 2.620(4) Å, respectively. The N5–N6 distance of 1.178(6) Å is only marginally distinct from the N6–N7 distance of 1.124(7) Å, which is in agreement with the range of reported bond lengths (1.187(5)–1.162(6) Å in U(Tren^{TIPS})(N₃) and 1.189(3)–1.153(3) Å in U(TIG)₃(N₃) (TIG = *N,N,N',N''*-tetrakispropylguanidinate)).^{17,63} This phenomenon suggests a slight preference of the N≡N⁺–N^{2–} resonance form for azide over the [–]N=N⁺=N[–] form, which might be induced by the coordination of the uranium ion, and also implies weak azide activation. The U1–N5 bond length of 2.293(4) Å is typical of that seen in U(Tren^{TIPS})(N₃) (2.305(3) Å) and U(TIG)₃(N₃) (2.3260(18) Å). Additionally, **5** exhibits an effective magnetic moment of 3.29 μ_B at 300 K, which decreases to 0.69 μ_B at 2 K (Figure 2). Although its magnetic behavior is consistent with the U(IV) oxidation state assignment, its magnetic moment at 300 K is appreciably higher than the reported values in the literature.^{30,64} ¹H NMR spectroscopy indicates that **5** exhibits C₃ symmetry, and resonance signals from –15 to +44 ppm assigned to 45 protons integrate properly. Although the assignment remains equivocal, a resonance at high field shifted to –9.77 ppm in comparison to **3** (–6.61 ppm) can be readily assigned to the TMS groups. The ²⁹Si NMR spectrum of **5** with a single resonance signal at

–197.31 ppm exhibits a shift of nearly –49 ppm in comparison to that of **3**. An alternative explanation is that an azide is a better electron donor in comparison with a chloride ion. Similarly to compound **4**, the FT-IR spectrum of **5** exhibits a strong absorption at 2081 cm^{–1} that is in consistent with a previously reported experimental value for a uranium(IV)–azide species (Figure S7).³⁰ The UV–vis–NIR spectrum of uranium(IV) complex **5** reveals multiple low-intensity adsorption bands and an optical adsorption spectrum with small extinction coefficients (ε = 10–50 M^{–1} cm^{–1}) between 500 and 2000 nm due to forbidden f–f transitions, with two relatively strong adsorption signals at around 680 and 1130 nm (Figure S8).

Having observed the ability for salt metathesis of a U(IV)–Cl bond to induce OCP and N₃, we were interested in its reduction chemistry. As we know, KC₈ is a classical reductant and has been extensively exploited to the fundamental reduction of uranium compounds.⁶⁵ Surprisingly, treatment of KC₈ with a precooled mixture of **3** generated, after workup and isolation, the oxo complex [(U(Trapen^{TMS}))₂(μ-O)] (**6**) as a dark yellow powder in 91% isolated yield. Attempts with other reductants, such as Na/Hg and Cp₂Co, to prepare the expected (Trapen^{TMS})U(III) derivative were also unsuccessful. According to the unexpected result mentioned above, it is possible that the oxo group in **6** most possibly originates from free THF solvent in the reaction system.⁶⁶ The X-ray single-crystal analysis of **6** reveals a μ-oxo-bridged and dinuclear structure featuring linear U–O–U (180.0°), bridging two five-coordinate uranium entities (Figure 1d). The U–O distance for **6** is 2.132(3) Å, and so the U–O distance is slightly shortened by almost 0.125 Å in comparison to that of 2.257(10) Å in **4**. The average U–N_{amido} distance in **6** is about 0.1 Å shorter than that in **3**, reflecting that the partial charge of the ligand migrates and accumulates at the uranium center. The effective magnetic moment for **6** is 4.30 μ_B per molecule (3.05 μ_B per uranium ion) at 300 K (Figure 2), as determined by SQUID magnetometry, which is comparable to the 3.16 μ_B reported for Meyer's oxo complex³⁴ but is well below the 3.54 μ_B expected for a free U(IV) ion.⁶⁷ Meanwhile, its magnetic moment is 1.38 μ_B per uranium ion at 2 K, fully consistent with the U(IV) oxidation state assignment.⁵¹ The ¹H NMR spectrum of **6** in solution is consistent with a C₃-symmetrical ligand environment and shows seven singlet signals at 105.30, 104.87, 34.70, 21.80, 8.23, –11.21, and –31.84 ppm. Of these, six peaks could be assigned to the aromatic skeleton and methylene protons in the Trapen ligand. The resonance of **6** in its ²⁹Si NMR spectrum exhibits a considerable shift in comparison to that of **3** at –250 ppm; this is shifted nearly –101 ppm from that of **3**. Other spectral and analytical data are consistent with the proposed structure for **6** (see the Supporting Information). The UV–vis–NIR spectrum of **6**, recorded in THF solution from 300 to 1600 nm, displays relatively prominent electronic transitions, which occur at 1185 and 1245 nm with low-intensity absorptivity values (49 and 26 M^{–1} cm^{–1}, respectively) for forbidden transitions. This is clearly in accord with the electronic absorption spectra observed for typical U(IV) complexes, further supporting a 5f² electronic configuration with a formal ³H₄ ground state (Figure S10).^{68,69}

To further understand the electronic structures of complexes **3**–**6**, we carried out quantum chemical calculations on the basis of their crystal structures. The detailed computation method is presented in the Supporting Information. The

optimized structures at the B3LYP/ECP/6-31G(d) level of theory in the gas phase are in agreement with the crystal data (Table S1), indicating that the level of theory used here is reliable and can provide the qualitative trend for these electronic structures. The natural spin density on the uranium for the complexes 3–6 is about 2.08 (Table S2), which is excellently consistent with a $5f^2$ configuration. The Wiberg bond indices (WBIs) of U–Cl (3), U–O (4), and U–N (5) bonds are 0.965, 0.540, and 0.713, respectively, as presented in Table S3. In addition, the two U–O WBIs for complex 6 are about 0.80, which indicates that the oxidation states of the two uranium atoms are equivalent. In addition, the frontier molecular orbitals of complex 6 have mainly $5f$ character and their energies are almost the same (Figure 3), in agreement with the U(IV) $5f^2$ character. Similar results were found for complexes 3–5 (Figure S11).

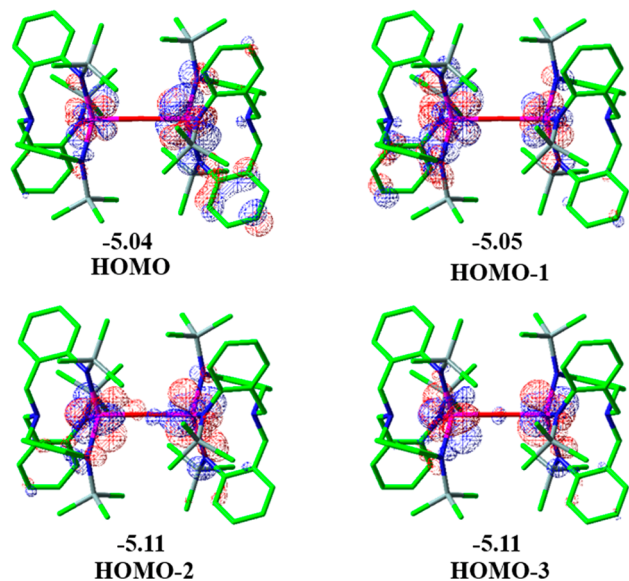


Figure 3. Frontier molecular orbitals of **6** and the corresponding orbital energies (eV). Orbital plots are generated with a contour value of 0.02 au.

CONCLUSION

In summary, we have designed and synthesized a novel tripodal Trapen ligand, and the corresponding reactive uranium(IV)–Cl complex anchored by the functionalized and sterically encumbering ligand Trapen has been constructed and proven to be sterically demanding and well suited for derivation. The set of uranium complexes $U(\text{Trapen}^{\text{TMS}})(\text{OCP})$ (**4**), $U(\text{Trapen}^{\text{TMS}})(\text{N}_3)$ (**5**), and $[\{U(\text{Trapen}^{\text{TMS}})\}_2(\mu\text{-O})]$ (**6**) with a U–O–U fragment was formed by straightforward conversion of the uranium(IV)–Cl precursor. The computational results confirm that these Trapen-based U(IV) complexes have $5f^2$ character. The outcome implies that Trapen could serve as an excellent and potential ligand worthy of further research and utilization.

EXPERIMENTAL SECTION

Caution! The uranium-containing compounds are radioactive and chemically toxic reactants. Precautions with suitable care and protection for handling such substances should be followed in the experiments.

General Methods. All air and moisture-sensitive experiments were conducted under a dry argon atmosphere using standard Schlenk techniques or a Vigor argon atmosphere glovebox (<1 ppm of O_2 ; <1 ppm of H_2O). Commercial reagents and solvents were purchased from J&K, Strem, Alfa Aesar, and others. Solvents were dried and degassed using a two-column solid-state purification system and stored in Young ampules over either a potassium mirror under argon or activated 4 Å molecular sieves (THF). C_6D_6 was distilled from Na/K, freeze–pump–thaw degassed, and stored under Ar. All NMR spectra were recorded on Bruker AVACNEIII HD 500 spectrometers at operating frequencies of 500 MHz for ^1H , 125 MHz for ^{13}C , 99 MHz for ^{29}Si , and 202 MHz for ^{31}P measurements. ^1H and ^{13}C chemical shifts were referenced (δ 0) internally to the residual solvent peaks of the deuterated solvent employed and are quoted relative to tetramethylsilane (TMS) as the internal standard at room temperature. The peak patterns are indicated as follows: s, singlet; d, doublet; t, triplet; m, multiplet; q, quartet. The coupling constants, J , are reported in hertz (Hz). Mass spectrometric measurements were recorded in positive ion mode using an amazon SL ion trap mass spectrometer (Bruker Daltonics, Bremen, Germany) and an electrospray interface as the ionization source. Magnetic susceptibility measurements on crystalline samples were carried out on a SQUID magnetometer at 0.1 T in the temperature range from 2 to 300 K. Single-crystal X-ray diffraction data of all compounds were collected on a Bruker D8 VENTURE X-ray CMOS diffractometer with a Mo $K\alpha$ X-ray source ($\lambda = 0.71073$ Å) or a Cu $K\alpha$ X-ray source ($\lambda = 1.54184$ Å) at 170 or 200 K. All of the crystal structures were solved by means of direct methods, refined with full-matrix least squares on SHELXL-97,⁷⁰ and refined with full-matrix least squares on SHELXL-2014.⁷¹ All non-hydrogen atoms were refined with anisotropic displacement parameters. Electronic absorption spectra were collected with a UV–vis–NIR spectrophotometer (Agilent Cary-5000). Infrared spectra of solid samples were recorded on a Bruker Tensor 27 instrument using KBr pellets, and infrared spectra of samples in THF solution were recorded using a KBr cell. Elemental analyses (C, H, N) were performed on a Vario EL III elemental analyzer at Peking University.

Synthesis of Bis(2-nitrobenzyl)amine (B). In a 500 mL round-bottom flask were placed 21.6 g (100 mmol) of 1-(bromomethyl)-2-nitrobenzene (A), 200 mL of ethanol, and 50.0 mL of ammonia. The mixture was stirred at room temperature for 2 days. During the course of the reaction, abundant needle crystals precipitated. After the reaction was complete, a light yellow solid was collected by filtration. The solid was dried to give the product **B** (10 g, 71% yield). ^1H NMR (500 MHz, CDCl_3): δ (ppm) 7.95 (d, $J = 8.1$ Hz, 2H), 7.57–7.63 (m, 4H), 7.42 (d, $J = 7.5$ Hz, 2H), 4.08 (s, 4H), 2.14 (s, 1H); ^{13}C NMR (125 Hz, CDCl_3): δ (ppm) 149.2, 135.2, 133.2, 131.2, 128.1, 124.8, 50.3. ESI-MS (m/z): $\text{C}_{14}\text{H}_{14}\text{N}_3\text{O}_4$ ($[\text{M} + \text{H}]^+$); found, m/z 288.2.

Synthesis of Tris(2-nitrobenzyl)amine (C). A 10.0 g portion (34.8 mmol) of bis(2-nitrobenzyl)amine (B) was dissolved in 100 mL of acetonitrile, to which was added 20.0 g of potassium carbonate. To the mixture was additionally added 7.5 g (35.0 mol) of 1-(bromomethyl)-2-nitrobenzene (A), and this mixture was heated to reflux for 48 h. After it was cooled to room temperature, the mixture was filtered and the filtrate was then evaporated to give the crude product, which was purified by recrystallization in CH_3CN to afford **C** (12.8 g, 87% yield). ^1H NMR (500 MHz, CDCl_3): δ (ppm) 7.80 (d, $J = 8.1$ Hz, 3H), 7.61 (d, $J = 7.7$ Hz, 3H), 7.54 (t, $J = 7.5$ Hz, 3H), 7.36 (t, $J = 7.7$ Hz, 3H), 3.94 (s, 6H). ^{13}C NMR (125 MHz, CDCl_3): δ (ppm) 149.6, 133.1, 132.9, 131.0, 128.2, 124.5, 56.0. ESI-MS (m/z): $\text{C}_{21}\text{H}_{19}\text{N}_4\text{O}_6$ ($[\text{M} + \text{H}]^+$); found, m/z 423.3.

Synthesis of 2-((Bis(2-aminobenzyl)amino)methyl)aniline (1). A 13.0 g portion (30.8 mmol) of tris(2-nitrobenzyl)amine (C) and Pd/C (1.0 g) were placed in a 250 mL round-bottom flask, and EtOH (100 mL) and hydrazine hydrate (30 mL) were added. The mixture was stirred at 50 °C for 0.5 h. The resulting mixture was cooled to room temperature and filtered by diatomaceous earth. The combined solvent was removed by a rotary evaporator, and the residue was purified by recrystallization from EtOH to afford **1** (henceforth Trapen) (9.1 g, 89% yield). ^1H NMR (500 MHz,

CDCl₃): δ (ppm) 7.07 (m, 6H), 6.67 (t, $J = 7.4$ Hz, 3H), 6.56 (d, $J = 8.2$ Hz, 3H), 3.96 (s, 6H), 3.46 (s, 6H). ¹³C NMR (125 MHz, CDCl₃): δ (ppm) 145.6, 132.0, 128.9, 121.9, 117.8, 115.5, 57.1. ESI-MS (m/z): C₂₁H₂₅N₄ ([M + H]⁺); found, m/z 333.2.

Synthesis of 2. *n*-BuLi (2.5 M, 4.0 mL, 10.0 mmol) was added dropwise to a precooled (−78 °C) solution of 2-((bis(2-aminobenzyl)amino)methyl)aniline (**1**; 1.1 g, 3.3 mmol) in THF (30 mL). The light yellow slurry was warmed to room temperature and stirred for a further 12 h. Then the solution was cooled to −78 °C and TMSCl (1.08 g, 10.0 mmol) was added. The solution was warmed to room temperature and stirred for 12 h. Volatiles were removed *in vacuo*, and the residue was extracted into hexane. The hexane solution was cooled to −78 °C again and *n*-BuLi (2.5 M, 4.0 mL, 10.0 mmol) was added. The solution was warmed to room temperature and stirred for 12 h. The solvent was removed *in vacuo* and the light yellow solid washed with hexanes (15 mL) to yield (Trapen^{TMS})(Li)₃ (**2**). Yield: 1.49 g, 80%. Crystalline material was obtained by dissolution of a small portion in toluene (5 mL) and storage at −30 °C. ¹H NMR (500 MHz, C₆D₆): δ (ppm) 7.10–7.14 (m, 3H), 6.97 (d, $J = 8.0$ Hz, 3H), 6.90–6.92 (m, 3H), 6.66 (t, $J = 7.3$ Hz, 3H), 4.08 (d, $J = 12.7$ Hz, 3H), 2.39 (d, $J = 12.5$ Hz, 3H), 0.2 (s, 27H). ¹³C NMR (125 MHz, C₆D₆): δ (ppm) 154.8, 134.2, 130.3, 125.5, 125.2, 117.2, 61.0, 1.9.

Synthesis of 3. A solution of UCl₄ (760.0 mg, 2.0 mmol) in THF (10 mL) was added to a precooled solution of (Trapen^{TMS})(Li)₃ (1.13 g, 2.0 mmol) in THF (10 mL) at −78 °C. The mixture turned black. The mixture was warmed to room temperature and stirred overnight. After the solvent was removed *in vacuo*, the product was extracted with toluene and filtered, yielding a black solution. The filtrate was stored at −78 °C and yielded complex **3** as yellow crystals. Yield: 1.01 g, 62%. ¹H NMR (500 MHz, C₆D₆, 298 K): δ (ppm) 21.37 (s, 3H), 20.53 (s, 3H), 11.30 (d, $J = 7.2$ Hz, 3H), 7.52 (t, $J = 6.7$ Hz, 3H), 3.71 (s, 3H), −2.92 (d, $J = 6.7$ Hz, 3H), −6.82 (s, 27H). ²⁹Si NMR (99 MHz, C₆D₆, 298 K): δ (ppm) −148.69. Anal. Calcd for C₃₀H₄₅ClN₄Si₃U: C, 43.97; H, 5.55; N, 6.84. Found: C, 43.79; H, 5.68; N, 6.73. FT-IR ν/cm^{-1} (KBr): 3380(w), 2957(m), 1591(m), 1469(m), 1246(s), 1045(m), 840(vs), 751(m), 701(m), 683(m), 475(m).

Synthesis of 4. THF (10 mL) was added slowly to a stirred mixture of [U(Trapen^{TMS})(Cl)] (819 mg, 1.0 mmol) and NaOCP(dioxane)_{2.5} (332.2 mg, 1.1 mmol) at −78 °C. The mixture was warmed to room temperature with stirring over 12 h. Volatiles were removed *in vacuo*, and the product was extracted into toluene (~10 mL). The mixture was filtered to remove the NaCl precipitate and remaining NaOCP(dioxane)_{2.5}, concentrated, and stored at −30 °C to yield yellow crystals of **4**. Yield: 0.65 g, 77%. Anal. Calcd for C₃₁H₄₅N₄OPSi₃U: C, 44.94; H, 5.67; N, 6.99. Found: C, 45.15; H, 5.58; N, 6.71. ¹H NMR (500 MHz, C₆D₆, 298 K): δ (ppm) 30.54 (s, 3H), 29.88 (s, 3H), 13.81 (d, $J = 8.0$ Hz, 3H), 7.66 (t, $J = 7.1$ Hz, 3H), −7.83 (d, $J = 7.1$ Hz, 3H), −9.66 (s, 27H, TMS), −31.19 (s, 3H). ²⁹Si NMR (C₆D₆, 298 K): not observed. ³¹P NMR (202 MHz, C₆D₆, 298 K): δ (ppm) −285.55. FT-IR ν/cm^{-1} (KBr): 3060(w), 2952(m), 1673(m), 1592(m), 1475(m), 1443(m), 1368(s), 1243(m), 1117(m), 1040(m), 907(m), 839(s), 750(m), 478(m).

Synthesis of 5. THF (10 mL) was added slowly to a stirred mixture of [U(Trapen^{TMS})(Cl)] (819 mg, 1.0 mmol) and NaN₃ (71.5 mg, 1.1 mmol) at −78 °C. The mixture was warmed to room temperature with stirring over 12 h. Volatiles were removed *in vacuo*, and the product was extracted into toluene (~15 mL). The mixture was filtered to remove the NaCl precipitate and remaining NaN₃, concentrated, and stored at −30 °C to yield yellow crystals of **5**. Yield: 0.57 g, 69%. Anal. Calcd for C₃₀H₄₅N₇Si₃U: C, 43.62; H, 5.50; N, 11.87. Found: C, 43.48; H, 5.39; N, 11.73. ¹H NMR (500 MHz, C₆D₆, 298 K): δ (ppm) 43.42 (s, 3H), 42.93 (s, 3H), 17.50 (d, $J = 7.0$ Hz, 3H), 7.92 (d, $J = 5.6$ Hz, 3H), −0.31 (s, 3H), −13.45 (s, 27H, TMS), −14.93 (s, 3H). ²⁹Si NMR (99 MHz, C₆D₆, 298 K): δ (ppm) −197.31. FT-IR ν/cm^{-1} : 3382(w), 2950(m), 2081(m), 1601(m), 1492(m), 1253(m), 906(m), 842(s), 751(m).

Synthesis of 6. In the drybox, crystals of **3** (819 mg, 1.0 mmol) were weighed into a 20 mL glass scintillation vial. The vial was

charged with ~5 mL of THF and a magnetic stir bar. The vial was then placed in a cooled cold well at −78 °C, and a suspension of KC₈ (46 mg, 0.4 mmol) in THF (1 mL) was added. The solution turned rapidly from yellow to black. The solution was stirred for 1 h at room temperature. Volatiles were removed *in vacuo*, and the product was extracted into toluene (~10 mL). The mixture was filtered to remove the graphite and KCl precipitate, concentrated, and stored at −30 °C to yield dark yellow crystals of **6**. Yield: 0.72 g, 91%. Anal. Calcd for C₆₀H₉₀ON₈Si₆U₂: C, 45.51; H, 5.39; N, 6.65. Found: C, 45.70; H, 5.61; N, 6.79. ¹H NMR (500 MHz, C₆D₆, 298 K): δ (ppm) 105.30 (s, 6H), 104.87 (s, 6H), 34.70 (s, 6H), 21.80 (s, 6H), 8.23 (s, 6H), −11.21 (s, 6H), −31.84 (s, 54H). ²⁹Si NMR (C₆D₆, 298 K): δ (ppm) −250.06. FT-IR ν/cm^{-1} : 3375(m), 2953(m), 1604(m), 1493(m), 1376(m), 1290(m), 1251(m), 1251(m), 905(m), 842(s), 751(m), 1251(m), 905(m), 842(s), 751(m).

■ ASSOCIATED CONTENT

Supporting Information

The Supporting Information is available free of charge at <https://pubs.acs.org/doi/10.1021/acs.organomet.0c00638>.

NMR, UV–vis–NIR, and IR spectroscopic data and computational details (PDF)

Accession Codes

CCDC 2003021–2003024 contain the supplementary crystallographic data for this paper. These data can be obtained free of charge via www.ccdc.cam.ac.uk/data_request/cif, or by emailing data_request@ccdc.cam.ac.uk, or by contacting The Cambridge Crystallographic Data Centre, 12 Union Road, Cambridge CB2 1EZ, UK; fax: +44 1223 336033.

■ AUTHOR INFORMATION

Corresponding Authors

Lei Mei – Laboratory of Nuclear Energy Chemistry, Institute of High Energy Physics, Chinese Academy of Sciences, Beijing 100049, People's Republic of China; orcid.org/0000-0002-2926-7265; Phone: 86-10-88235242; Email: meil@ihep.ac.cn

Wei-Qun Shi – Laboratory of Nuclear Energy Chemistry, Institute of High Energy Physics, Chinese Academy of Sciences, Beijing 100049, People's Republic of China; orcid.org/0000-0001-9929-9732; Phone: 86-10-88233968; Email: shiwq@ihep.ac.cn

Authors

Kang Liu – Laboratory of Nuclear Energy Chemistry, Institute of High Energy Physics, Chinese Academy of Sciences, Beijing 100049, People's Republic of China; University of Chinese Academy of Sciences, Beijing 100039, China

Ji-Pan Yu – Laboratory of Nuclear Energy Chemistry, Institute of High Energy Physics, Chinese Academy of Sciences, Beijing 100049, People's Republic of China

Qun-Yan Wu – Laboratory of Nuclear Energy Chemistry, Institute of High Energy Physics, Chinese Academy of Sciences, Beijing 100049, People's Republic of China

Xue-Bing Tao – College of Chemistry and Chemical Engineering, University of South China, Hengyang 421001, People's Republic of China

Xiang-He Kong – College of Chemistry and Chemical Engineering, University of South China, Hengyang 421001, People's Republic of China

Kong-Qiu Hu – Laboratory of Nuclear Energy Chemistry, Institute of High Energy Physics, Chinese Academy of Sciences, Beijing 100049, People's Republic of China

Li-Yong Yuan – Laboratory of Nuclear Energy Chemistry, Institute of High Energy Physics, Chinese Academy of Sciences, Beijing 100049, People's Republic of China; orcid.org/0000-0003-4261-8717

Zhi-Fang Chai – Laboratory of Nuclear Energy Chemistry, Institute of High Energy Physics, Chinese Academy of Sciences, Beijing 100049, People's Republic of China; Engineering Laboratory of Advanced Energy Materials, Ningbo Institute of Industrial Technology, Chinese Academy of Sciences, Ningbo, Zhejiang 315201, People's Republic of China

Complete contact information is available at:
<https://pubs.acs.org/10.1021/acs.organomet.0c00638>

Author Contributions

¹K.L. and J.-P.Y. contributed equally to this work.

Notes

The authors declare no competing financial interest.

ACKNOWLEDGMENTS

This work was supported by the National Natural Science Foundation of China (Grant Nos. 21806167), the National Science Fund for Distinguished Young Scholars (No. 21925603), and the Science Challenge Project (TZ2016004).

REFERENCES

- (1) Liddle, S. T. The Renaissance of Non-Aqueous Uranium Chemistry. *Angew. Chem., Int. Ed.* **2015**, *54*, 8604–8641.
- (2) Scott, P.; Hitchcock, P. B. Synthesis of Tripodal Amido Complexes of the Early Actinides; Molecular Structure of (N-[CH₂CH₂N(SiMe₃)₃UCl])₂. *Polyhedron* **1994**, *13*, 1651–1653.
- (3) Roussel, P.; Scott, P. Complex of dinitrogen with trivalent uranium. *J. Am. Chem. Soc.* **1998**, *120*, 1070–1071.
- (4) Gardner, B. M.; Liddle, S. T. Uranium triamidoamine chemistry. *Chem. Commun.* **2015**, *51*, 10589–10607.
- (5) Liddle, S. T.; McMaster, J.; Mills, D. P.; Blake, A. J.; Jones, C.; Woodul, W. D. σ and π Donation in an Unsupported Uranium-Gallium Bond. *Angew. Chem., Int. Ed.* **2009**, *48*, 1077–1080.
- (6) Ward, A. L.; Lukens, W. W.; Lu, C. C.; Arnold, J. Photochemical Route to Actinide-Transition Metal Bonds: Synthesis, Characterization and Reactivity of a Series of Thorium and Uranium Heterobimetallic Complexes. *J. Am. Chem. Soc.* **2014**, *136*, 3647–3654.
- (7) Patel, D.; Lewis, W.; Blake, A. J.; Liddle, S. T. Uranium(IV) amide and halide derivatives of two tripodal tris(N-arylamido-dimethylsilyl)methanes. *Dalton Trans.* **2010**, *39*, 6638–6647.
- (8) Patel, D.; Moro, F.; McMaster, J.; Lewis, W.; Blake, A. J.; Liddle, S. T. A Formal High Oxidation State Inverse-Sandwich Diuranium Complex: A New Route to f-Block-Metal Bonds. *Angew. Chem., Int. Ed.* **2011**, *50*, 10388–10392.
- (9) Patel, D.; King, D. M.; Gardner, B. M.; McMaster, J.; Lewis, W.; Blake, A. J.; Liddle, S. T. Structural and theoretical insights into the perturbation of uranium-rhenium bonds by dative Lewis base ancillary ligands. *Chem. Commun.* **2011**, *47*, 295–297.
- (10) Gardner, B. M.; Patel, D.; Cornish, A. D.; McMaster, J.; Lewis, W.; Blake, A. J.; Liddle, S. T. The Nature of Unsupported Uranium-Ruthenium Bonds: A Combined Experimental and Theoretical Study. *Chem. - Eur. J.* **2011**, *17*, 11266–11273.
- (11) Patel, D.; Tuna, F.; McInnes, E. J. L.; Lewis, W.; Blake, A. J.; Liddle, S. T. An Actinide Zintl Cluster: A Tris(triamidouranium) μ_3 - η^2 : η^2 : η^2 -Heptaphosphanortricyclane and Its Diverse Synthetic Utility. *Angew. Chem., Int. Ed.* **2013**, *52*, 13334–13337.
- (12) Gardner, B. M.; Kefalidis, C. E.; Lu, E.; Patel, D.; McInnes, E. J. L.; Tuna, F.; Wooles, A. J.; Maron, L.; Liddle, S. T. Evidence for single metal two electron oxidative addition and reductive elimination at uranium. *Nat. Commun.* **2017**, *8*, 1898.
- (13) Lam, O. P.; Anthon, C.; Meyer, K. Influence of steric pressure on the activation of carbon dioxide and related small molecules by uranium coordination complexes. *Dalton Trans.* **2009**, *44*, 9677–9691.
- (14) Du, J. Z.; Alvarez-Lamsfus, C.; Wildman, E. P.; Wooles, A. J.; Maron, L.; Liddle, S. T. Thorium-nitrogen multiple bonds provide evidence for pushing-from-below for early actinides. *Nat. Commun.* **2019**, *10*, 4203.
- (15) Du, J. Z.; King, D. M.; Chatelain, L.; Lu, E. L.; Tuna, F.; McInnes, E. J. L.; Wooles, A. J.; Maron, L.; Liddle, S. T. Thorium- and uranium-azide reductions: a transient dithorium-nitride versus isolable diuranium-nitrides. *Chem. Sci.* **2019**, *10*, 3738–3745.
- (16) Magnall, R.; Balazs, G.; Lu, E. L.; Kern, M.; van Slageren, J.; Tuna, F.; Wooles, A. J.; Scheer, M.; Liddle, S. T. Photolytic and Reductive Activations of 2-Arsaethynolate in a Uranium-Triamidoamine Complex: Decarbonylative Arsenic-Group Transfer Reactions and Trapping of a Highly Bent and Reduced Form. *Chem. - Eur. J.* **2019**, *25*, 14246–14252.
- (17) Magnall, R.; Balazs, G.; Lu, E. L.; Tuna, F.; Wooles, A. J.; Scheer, M.; Liddle, S. T. Trapping of a Highly Bent and Reduced Form of 2-Phosphaethynolate in a Mixed-Valence Diuranium-Triamidoamine Complex. *Angew. Chem., Int. Ed.* **2019**, *58*, 10215–10219.
- (18) Wildman, E. P.; Balazs, G.; Wooles, A. J.; Scheer, M.; Liddle, S. T. Triamidoamine thorium-arsenic complexes with parent arsenide, arsinide and arsenido structural motifs. *Nat. Commun.* **2017**, *8*, 14769.
- (19) Gardner, B. M.; King, D. M.; Tuna, F.; Wooles, A. J.; Chilton, N. F.; Liddle, S. T. Assessing crystal field and magnetic interactions in diuranium- μ -chalcogenide triamidoamine complexes with U^{IV}-E-U^{IV} cores (E = S, Se, Te): implications for determining the presence or absence of actinide-actinide magnetic exchange. *Chem. Sci.* **2017**, *8*, 6207–6217.
- (20) Rookes, T. M.; Gardner, B. M.; Balazs, G.; Gregson, M.; Tuna, F.; Wooles, A. J.; Scheer, M.; Liddle, S. T. Crystalline Diuranium Phosphinidide and μ -Phosphido Complexes with Symmetric and Asymmetric UPU Cores. *Angew. Chem., Int. Ed.* **2017**, *56*, 10495–10500.
- (21) Wildman, E. P.; Balazs, G.; Wooles, A. J.; Scheer, M.; Liddle, S. T. Thorium-phosphorus triamidoamine complexes containing Th-P single- and multiple-bond interactions. *Nat. Commun.* **2016**, *7*, 12884.
- (22) King, D. M.; Cleaves, P. A.; Wooles, A. J.; Gardner, B. M.; Chilton, N. F.; Tuna, F.; Lewis, W.; McInnes, E. J. L.; Liddle, S. T. Molecular and electronic structure of terminal and alkali metal-capped uranium(V) nitride complexes. *Nat. Commun.* **2016**, *7*, 13773.
- (23) Brown, J. L.; Gaunt, A. J.; King, D. M.; Liddle, S. T.; Reilly, S. D.; Scott, B. L.; Wooles, A. J. Neptunium and plutonium complexes with a sterically encumbered triamidoamine (TREN) scaffold. *Chem. Commun.* **2016**, *52*, 5428–5431.
- (24) Gardner, B. M.; Balazs, G.; Scheer, M.; Tuna, F.; McInnes, E. J. L.; McMaster, J.; Lewis, W.; Blake, A. J.; Liddle, S. T. Triamidoamine uranium(IV)-arsenic complexes containing one-, two- and threefold U-As bonding interactions. *Nat. Chem.* **2015**, *7*, 582–590.
- (25) Gardner, B. M.; Balazs, G.; Scheer, M.; Wooles, A. J.; Tuna, F.; McInnes, E. J. L.; McMaster, J.; Lewis, W.; Blake, A. J.; Liddle, S. T. Isolation of Elusive HAsAsH in a Crystalline Diuranium(IV) Complex. *Angew. Chem., Int. Ed.* **2015**, *54*, 15250–15254.
- (26) Gardner, B. M.; Tuna, F.; McInnes, E. J. L.; McMaster, J.; Lewis, W.; Blake, A. J.; Liddle, S. T. An Inverted-Sandwich Diuranium μ - η^5 : η^5 -Cyclo-P₅ Complex Supported by U-P₅ δ -Bonding. *Angew. Chem., Int. Ed.* **2015**, *54*, 7068–7072.
- (27) King, D. M.; McMaster, J.; Tuna, F.; McInnes, E. J. L.; Lewis, W.; Blake, A. J.; Liddle, S. T. Synthesis and Characterization of an f-Block Terminal Parent Imido [U = NH] Complex: A Masked Uranium(IV) Nitride. *J. Am. Chem. Soc.* **2014**, *136*, 5619–5622.
- (28) Gardner, B. M.; Balazs, G.; Scheer, M.; Tuna, F.; McInnes, E. J. L.; McMaster, J.; Lewis, W.; Blake, A. J.; Liddle, S. T. Triamidoamine-Uranium(IV)-Stabilized Terminal Parent Phosphide and Phosphinidene Complexes. *Angew. Chem., Int. Ed.* **2014**, *53*, 4484–4488.

- (29) Cleaves, P. A.; King, D. M.; Kefalidis, C. E.; Maron, L.; Tuna, F.; McInnes, E. J. L.; McMaster, J.; Lewis, W.; Blake, A. J.; Liddle, S. T. Two-Electron Reductive Carbonylation of Terminal Uranium(V) and Uranium(VI) Nitrides to Cyanate by Carbon Monoxide. *Angew. Chem., Int. Ed.* **2014**, *53*, 10412–10415.
- (30) King, D. M.; Tuna, F.; McInnes, E. J. L.; McMaster, J.; Lewis, W.; Blake, A. J.; Liddle, S. T. Isolation and characterization of a uranium(VI)-nitride triple bond. *Nat. Chem.* **2013**, *5*, 482–488.
- (31) King, D. M.; Tuna, F.; McInnes, E. J. L.; McMaster, J.; Lewis, W.; Blake, A. J.; Liddle, S. T. Synthesis and Structure of a Terminal Uranium Nitride Complex. *Science* **2012**, *337*, 717–720.
- (32) Hoerger, C. J.; Heinemann, F. W.; Louyriac, E.; Rigo, M.; Maron, L.; Grutzmacher, H.; Driess, M.; Meyer, K. Cyaarside (CAs⁻) and 1,3-Diarsaallendiide (AsCAs²⁻) Ligands Coordinated to Uranium and Generated via Activation of the Arsaethynolate Ligand (OCAs⁻). *Angew. Chem., Int. Ed.* **2019**, *58*, 1679–1683.
- (33) Halter, D. P.; Heinemann, F. W.; Maron, L.; Meyer, K. The role of uranium-arene bonding in H₂O reduction catalysis. *Nat. Chem.* **2018**, *10*, 259–267.
- (34) Hoerger, C. J.; Heinemann, F. W.; Louyriac, E.; Maron, L.; Grutzmacher, H.; Meyer, K. Formation of a Uranium-Bound η^1 -Cyaphide (CP⁻) Ligand via Activation and C-O Bond Cleavage of Phosphaethynolate (OCP⁻). *Organometallics* **2017**, *36*, 4351–4354.
- (35) Halter, D. P.; Heinemann, F. W.; Bachmann, J.; Meyer, K. Uranium-mediated electrocatalytic dihydrogen production from water. *Nature* **2016**, *530*, 317–323.
- (36) Rosenzweig, M. W.; Scheurer, A.; Lamsfus, C. A.; Heinemann, F. W.; Maron, L.; Andrez, J.; Mazzanti, M.; Meyer, K. Uranium(IV) terminal hydrosulfido and sulfido complexes: insights into the nature of the uranium-sulfur bond. *Chem. Sci.* **2016**, *7*, 5857–5866.
- (37) Schmidt, A. C.; Heinemann, F. W.; Lukens, W. W.; Meyer, K. Molecular and Electronic Structure of Dinuclear Uranium Bis- μ -Oxo Complexes with Diamond Core Structural Motifs. *J. Am. Chem. Soc.* **2014**, *136*, 11980–11993.
- (38) Franke, S. M.; Heinemann, F. W.; Meyer, K. Reactivity of uranium(IV) bridged chalcogenido complexes U^{IV}-E-U^{IV} (E = S, Se) with elemental sulfur and selenium: synthesis of polychalcogenido-bridged uranium complexes. *Chem. Sci.* **2014**, *5*, 942–950.
- (39) La Pierre, H. S.; Scheurer, A.; Heinemann, F. W.; Hieringer, W.; Meyer, K. Synthesis and Characterization of a Uranium(II) Monoarene Complex Supported by delta Backbonding. *Angew. Chem., Int. Ed.* **2014**, *53*, 7158–7162.
- (40) La Pierre, H. S.; Kameo, H.; Halter, D. P.; Heinemann, F. W.; Meyer, K. Coordination and Redox Isomerization in the Reduction of a Uranium(III) Monoarene Complex. *Angew. Chem., Int. Ed.* **2014**, *53*, 7154–7157.
- (41) Kosog, B.; La Pierre, H. S.; Heinemann, F. W.; Liddle, S. T.; Meyer, K. Synthesis of Uranium(VI) Terminal Oxo Complexes: Molecular Geometry Driven by the Inverse Trans-Influence. *J. Am. Chem. Soc.* **2012**, *134*, 5284–5289.
- (42) Lam, O. P.; Franke, S. M.; Heinemann, F. W.; Meyer, K. Reactivity of U-E-U (E = S, Se) Toward CO₂, CS₂, and COS: New Mixed-Carbonate Complexes of the Types U-CO₂E-U (E = S, Se), U-CS₂E-U (E = O, Se), and U-COSSe-U. *J. Am. Chem. Soc.* **2012**, *134*, 16877–16881.
- (43) Lam, O. P.; Heinemann, F. W.; Meyer, K. C-C Bond Formation through Reductive Coupling of CS₂ to Yield Uranium Tetrathiooxalate and Ethylenetetrathiolate Complexes. *Angew. Chem., Int. Ed.* **2011**, *50*, 5965–5968.
- (44) Zuend, S. J.; Lam, O. P.; Heinemann, F. W.; Meyer, K. Carbon Dioxide Insertion into Uranium-Activated Dicarboxyl Complexes. *Angew. Chem., Int. Ed.* **2011**, *50*, 10626–10630.
- (45) Winston, M. S.; Batista, E. R.; Yang, P.; Tondreau, A. M.; Boncella, J. M. Extending Stannyl Anion Chemistry to the Actinides: Synthesis and Characterization of a Uranium-Tin Bond. *Inorg. Chem.* **2016**, *55*, 5534–5539.
- (46) Gardner, B. M.; McMaster, J.; Moro, F.; Lewis, W.; Blake, A. J.; Liddle, S. T. An Unsupported Uranium-Rhenium Complex Prepared by Alkane Elimination. *Chem. - Eur. J.* **2011**, *17*, 6909–6912.
- (47) Feng, G. F.; Zhang, M. X.; Shao, D.; Wang, X. Y.; Wang, S. A.; Maron, L.; Zhu, C. Q. Transition-metal-bridged bimetallic clusters with multiple uranium-metal bonds. *Nat. Chem.* **2019**, *11*, 248–253.
- (48) Feng, G. F.; Zhang, M. X.; Wang, P. L.; Wang, S.; Maron, L.; Zhu, C. Q. Identification of a uranium-rhodium triple bond in a heterometallic cluster. *Proc. Natl. Acad. Sci. U. S. A.* **2019**, *116*, 17654–17658.
- (49) Halter, D. P.; Heinemann, F. W.; Bachmann, J.; Meyer, K. Uranium-mediated electrocatalytic dihydrogen production from water. *Nature* **2016**, *530*, 317–323.
- (50) Fox, A. R.; Bart, S. C.; Meyer, K.; Cummins, C. C. Towards uranium catalysts. *Nature* **2008**, *455*, 341–349.
- (51) Lam, O. P.; Feng, P. L.; Heinemann, F. W.; O'Connor, J. M.; Meyer, K. Charge-Separation in Uranium Diazomethane Complexes Leading to C-H Activation and Chemical Transformation. *J. Am. Chem. Soc.* **2008**, *130*, 2806–2816.
- (52) Cheisson, T.; Kersey, K. D.; Mahieu, N.; McSkimming, A.; Gau, M. R.; Carroll, P. J.; Schelter, E. J. Multiple Bonding in Lanthanides and Actinides: Direct Comparison of Covalency in Thorium(IV)- and Cerium(IV)-Imido Complexes. *J. Am. Chem. Soc.* **2019**, *141*, 9185–9190.
- (53) Alajarin, M.; Pastor, A.; Orenes, R.; Steed, J. W.; Arakawa, R. Self-Assembly of Tris(2-ureidobenzyl)amines: A New Type of Capped, Capsule-Like Dimeric Aggregates Derived from a Highly Flexible Skeleton. *Chem. - Eur. J.* **2004**, *10*, 1383–1397.
- (54) Windorff, C. J.; Evans, W. J. ²⁹Si NMR Spectra of Silicon-Containing Uranium Complexes. *Organometallics* **2014**, *33*, 3786–3791.
- (55) Addison, A. W.; Rao, T. N.; Reedijk, J.; van Rijn, J.; Verschoor, G. C. Synthesis, structure, and spectroscopic properties of copper(II) compounds containing nitrogen-sulphur donor ligands; the crystal and molecular structure of aqua[1,7-bis(N-methylbenzimidazol-2'-yl)-2,6-dithiaheptane]copper(II) perchlorate. *J. Chem. Soc., Dalton Trans.* **1984**, *7*, 1349–1356.
- (56) Berthet, J. C.; Ephritikhine, M. New advances in the chemistry of uranium amide compounds. *Coord. Chem. Rev.* **1998**, *178*, 83–116.
- (57) Castro-Rodriguez, I.; Nakai, H.; Meyer, K. Multiple-bond metathesis mediated by sterically pressured uranium complexes. *Angew. Chem., Int. Ed.* **2006**, *45*, 2389–2392.
- (58) Morris, D. E.; Da Re, R. E.; Jantunen, K. C.; Castro-Rodriguez, I.; Kiplinger, J. L. Trends in electronic structure and redox energetics for early-actinide pentamethylcyclopentadienyl complexes. *Organometallics* **2004**, *23*, 5142–5153.
- (59) Falivene, L.; Cao, Z.; Petta, A.; Serra, L.; Poater, A.; Oliva, R.; Scarano, V.; Cavallo, L. Towards the online computer-aided design of catalytic pockets. *Nat. Chem.* **2019**, *11*, 872–879.
- (60) Poater, A.; Ragone, F.; Giudice, S.; Costabile, C.; Dorta, R.; Nolan, S. P.; Cavallo, L. Thermodynamics of N-heterocyclic carbene dimerization: The balance of sterics and electronics. *Organometallics* **2008**, *27*, 2679–2681.
- (61) Poater, A.; Ragone, F.; Mariz, R.; Dorta, R.; Cavallo, L. Comparing the Enantioselective Power of Steric and Electrostatic Effects in Transition-Metal-Catalyzed Asymmetric Synthesis. *Chem. - Eur. J.* **2010**, *16*, 14348–14353.
- (62) Camp, C.; Settineri, N.; Lefevre, J.; Jupp, A. R.; Goicoechea, J. M.; Maron, L.; Arnold, J. Uranium and thorium complexes of the phosphoethynolate ion. *Chem. Sci.* **2015**, *6*, 6379–6384.
- (63) Settineri, N. S.; Shiau, A. A.; Arnold, J. Two-electron oxidation of a homoleptic U(III) guanidinate complex by diphenyldiazomethane. *Chem. Commun.* **2018**, *54*, 10913–10916.
- (64) Wildman, E. P.; Ostrowski, J. P. A.; King, D. M.; Lewis, W.; Liddle, S. T. Uranium-Halide and -Azide Derivatives of the Sterically Demanding Triamidoamine Ligand Tren^{TPS} [Tren^{TPS} = {N-(CH₂CH₂NSiPh₃)₃}³⁻]. *Polyhedron* **2017**, *125*, 2–8.
- (65) MacDonald, M. R.; Fieser, M. E.; Bates, J. E.; Ziller, J. W.; Furche, F.; Evans, W. J. Identification of the + 2 Oxidation State for Uranium in a Crystalline Molecular Complex, [K(2.2.2-Cryptand)]-[(C₅H₄SiMe₃)₃U]. *J. Am. Chem. Soc.* **2013**, *135*, 13310–13313.

(66) Gardner, B. M.; Lewis, W.; Blake, A. J.; Liddle, S. T. Halide, Amide, Cationic, Manganese Carbonylate, and Oxide Derivatives of Triamidodisilylamine Uranium Complexes. *Inorg. Chem.* **2011**, *50*, 9631–9641.

(67) Castro-Rodriguez, I.; Olsen, K.; Gantzel, P.; Meyer, K. Uranium Tris-aryloxy Derivatives Supported by Triazacyclononane: Engendering a Reactive Uranium(III) Center with a Single Pocket for Reactivity. *J. Am. Chem. Soc.* **2003**, *125*, 4565–4571.

(68) Graves, C. R.; Schelter, E. J.; Cantat, T.; Scott, B. L.; Kiplinger, J. L. A Mild Protocol To Generate Uranium(IV) Mixed-Ligand Metallocene Complexes using Copper(I) Iodide. *Organometallics* **2008**, *27*, 5371–5378.

(69) Kindra, D. R.; Evans, W. J. Magnetic Susceptibility of Uranium Complexes. *Chem. Rev.* **2014**, *114*, 8865–8882.

(70) Sheldrick, G. M. A short history of SHELX. *Acta Crystallogr., Sect. A: Found. Crystallogr.* **2008**, *64*, 112–122.

(71) Sheldrick, G. M. SHELXT-Integrated Space-Group and Crystal-Structure Determination. *Acta Crystallogr., Sect. A: Found. Adv.* **2015**, *71*, 3–8.